Research article

Impregnation of different lanthanides in a covalent organic framework (RIO-55) to a chemical determination of dopants substances

André Carvalho [a,b], Luis C. Branco [b], Leticia R.C. Corrêa [c], Ana B. Paninho [b], Pierre M. Esteves [c], Hugo Cruz [b,**], Sunny K.S. Freitas [b,*]

[a] *Escola Superior de Tecnologia do Barreiro, Rua Américo da Silva Marinho, s/n, 2839-001, Lavradio, Portugal*
[b] *LAQV-REQUIMTE, Department of Chemistry, NOVA School of Science and Technology, NOVA University of Lisbon, Campus de Caparica, 2829-516 Caparica, Portugal*
[c] *Instituto de Química, Universidade Federal do Rio de janeiro, Avenida Athos da Silveira Ramos, 149, CT A-622, Cidade Universitária, Ilha do Fundão, Rio de Janeiro 21941-909, Brazil*

A R T I C L E   I N F O

A B S T R A C T

Ionic Covalent Organic Frameworks are a special subgroup that has risen as promising materials for innovative applications. In parallel, some of the so-called Reticular Innovative Organic compounds (RIOs), which are ionic and non-ionic porous materials have been used with great versatility, for several purposes. In this work, the ionic dye-based RIO-55 was chosen to capture a series of lanthanides (Eu, Gd, Dy, and Tb) from water, observing their affinity with the lattice and the performance of the adsorbent. Thus, the higher adsorbed amount was referred to as Eu^{3+} ($Q_{max} = 370$ mg/g), as well as the best affinity ($K_L = 5x10^{-3}$), following the Langmuir model. The impregnated Eu^{3+}@RIO-55 was used for chemical sensing, capturing dopant molecules (ephedrine and dopamine) from water, showing great performance, even after some reuse cycles. In addition, some initial fluorescence tests were performed using RIO-55 and Eu^{3+}@RIO-55 to observe the spectrum before and after lanthanide impregnation.

1. Introduction

Lanthanides are an interesting class of elements due to their high reactivity, being used for various purposes, converging to the areas of health and imaging [1,2]. Lanthanide-based materials have been increasingly explored [3], especially in electroluminescent devices [4], as components of fuel cells [5], microelectronics [6], liquid crystal displays [7], etc. With this, these compounds have generated a considerable amount of waste that stays in the environment [8]. The common use of these elements in new technological products has resulted in significant changes in natural environmental processes, especially due to the increase in mining [9].

The search for materials that capture pollutants from water, soil, or air has been growing, due to the protocols established worldwide [10,11]. However, using these materials for a more targeted purpose is an advantage of some of these compounds, especially the porous ones. This class covers a wide variety of multifunctional materials, which can be used in a single approach for

---

different purposes, as adsorbents for different fluids that, by impregnation, form new functionalized materials [12]. These new functions enlarge the number of applications, generally improving the physicochemical characteristics of the original material [13,14]. A special and most robust class of porous materials, called Covalent Organic Frameworks (COFs), has been shown to be versatile, which makes them widely used in the most diverse purposes, especially in technologies related to environment and energy [15–21]. COFs and their derivatives (Covalent Organic Networks/Nanosheets, Porous Organic Polymers, among others) can be subdivided into ionic or non-ionic [22–24]. The ionic porous materials have been little reported, even though they have great potential for innovative applications, such as sensing, solid-state electrolytes, selective gas capture, etc. Reticular Innovative Organic frameworks (RIOs) are part of a subclass that integrates compounds with high and low crystallinity and different topologies, presenting 2D and 3D cross-linked materials with high porosity and great surface area values [25,26].

Here, we relate the efficiency of the pre-reported ionic porous material RIO-55[22] in the adsorption of some lanthanides, named europium (Eu^{3+}), gadolinium (Gd^{3+}), dysprosium (Dy^{3+}), and terbium (Tb^{3+}) from water. These metals are widely used as contrast agents, optical products, catalytic systems, etc [27]. Despite they are not considered toxic elements, many adsorption and recovery studies have been carried out, mainly for the industrial area [9]. The mesopores of RIO-55 work as good hosts for ions and molecules in a significant amount. Besides, its chemical functions in the pores and the lattice contribute to several interactions [28]. Once impregnated in the pores of the material (lanthanides@RIO-55), these elements favored the increase in the emission band of the compound, being good candidates for fluorescence sensors. Furthermore, Eu^{3+}@RIO-55 was chosen for detection tests of substances used in doping (ephedrine and dopamine). In the case of competitive sports, ephedrine has been used to improve exercise tolerance and prevent fatigue, in addition to accelerating the metabolism [29]. In turn, dopamine acts as a neurotransmitter and an excessive amount in the body can lead to several serious problems and may not be reversed [30]. Metal-modified COFs commonly increase the capacity of interaction with other molecules, ions, fluids, etc [31]. The formed interactions facilitate other impregnations by promoting a more robust system. This method validated the good efficiency of RIO-55 and the improvement of its performance after introducing europium into the pores and the lattice (Eu^{3+}@RIO-55).

2. Methods

2.1. Synthesis and characterization

RIO-55 was synthesized as presented in the literature [16]. In short, 125 mg (0.30 mmol) of the dye Bismark brown Y (Sigma Aldrich, 85 %) and 110 mg (0.52 mmol) of triformylphloroglucinol were added to a high-pressure vessel (ChemGlass, 48 mL). Then, 1, 4-dioxane was added (10 mL), followed by HOAc 6M (3 mL). The reaction remained under stirring and heating (120°) for 3 days. After this, the product obtained was a reddish powder, being dried by supercritical CO_2 (scCO$_2$) and characterized by FTIR-ATR, ^{13}C NMR (CP-MAS), PXRD, TGA, and N_2 adsorption/desorption (see ESI).

3. Lanthanides adsorption

The solutions containing lanthanide salts (hexahydrates $EuCl_3$, $GdCl_3$, $TbCl_3$, and $DyCl_3$) were prepared in Milli-Q water, ranging from 50 to 500 ppm. Then, 4 mg of RIO-55 was left in contact with 4 mL of the solution, with different concentrations, at a fixed temperature (24°C). These mixtures remained in a shaker (2400 rpm) for 24h. After this period, the suspensions were filtered with filters attached to syringes (PTFE membrane, 25 mm, 0.45 μm). The resulting solutions were analyzed by ICP (Inductively Coupled Plasma-Atomic Emission Spectrometer, Horiba Jobin-Yvon, Ultima). Thus, it is possible to quantify the final concentration of the solution and calculate the maximum amount adsorbed (Q_{max}) by difference method ($C_{initial}$-C_{final}) using the Langmuir parameters. Adsorption curves for each one of the metals were obtained by plotting Q_e (amount adsorbed in the equilibrium) versus C_e (final concentration), following the Langmuir model. From its non-linearized form, it was obtained Q_{max} (Q_e/C_e versus C_e), with an $R^2 > 0.9$ (see ESI). During this step, it was made same assays with different pH values (2.5–8.5), due to the influence of the medium on the adsorption. In this way, some solutions of $EuCl_3$ 100 ppm were used, following the same methodology described above.

4. Selectivity

Tests of lanthanide adsorption in competitive solutions were realized to observe the selectivity between the ions and the porous network. Solutions of 100 ppm of each lanthanide studied in this work were prepared (1 mL for each one). Then, 4 mg of RIO-55 was added to the final solution and replaced under stirring in a shaker for 4h. After this, the material was filtered, and the liquid was analyzed by ICP.

4.1. Fluorescence sensing analysis

Since lanthanides emit fluorescence, RIO-55 impregnated with europium (Eu^{3+}@RIO-55) was selected to be analyzed as a solid sensor. Tests were carried out using a Horiba-Jobin-Yvon SPEX Fluorolog 3.22 spectrofluorometer, adapted for assays in the solid state. Firstly, an emission spectrum for RIO-55 was obtained, exciting the sample at 320 nm. Then, the same was made for Eu^{3+}@RIO-55, to observe the difference between the emission bands after metal impregnation.
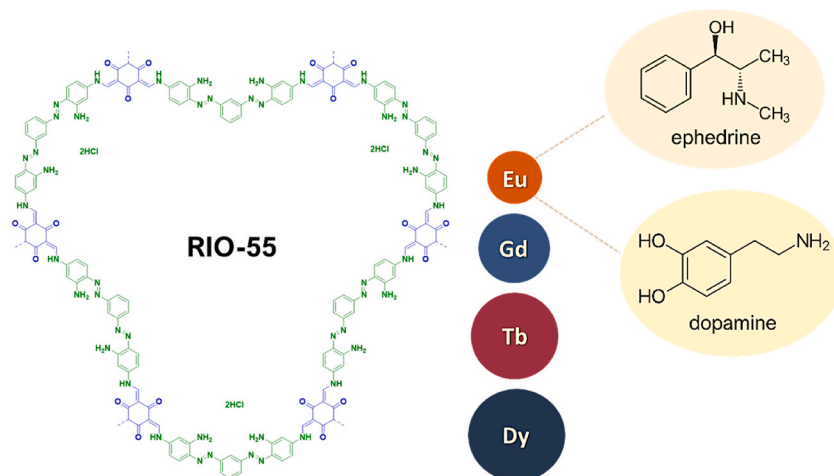
Fig. 1. Pore representation for RIO-55 (porous adsorbent), the lanthanides used in this study, and the doping substances.
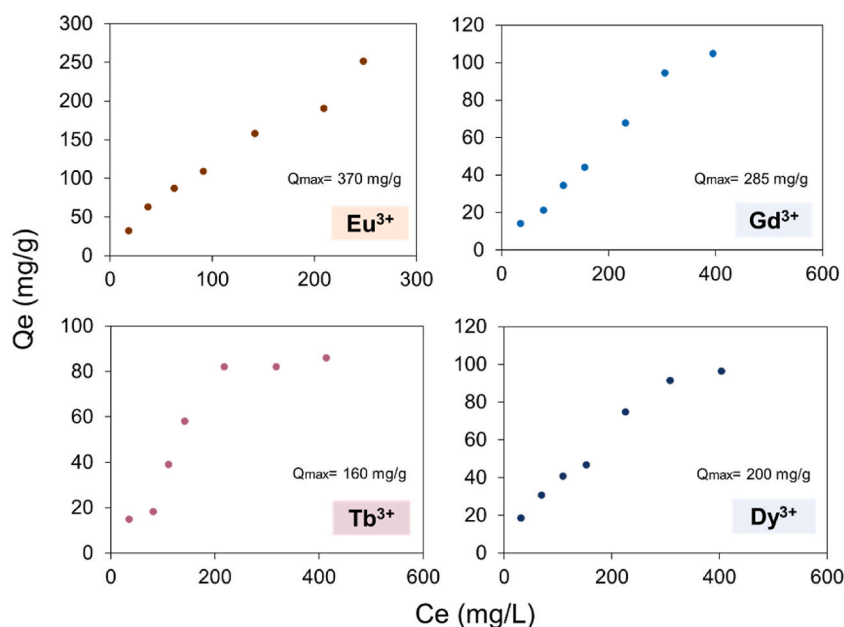

Fig. 2. Lanthanides adsorption isotherms for RIO-55, following the Langmuir model. The highest adsorbed amount is referred to Eu^{3+} with a Q_{max} = 370 mg/g.

4.2. Adsorption of doping substances

Aiming to direct a final application to the porous solids reported here, doping substances were selected to be detected. Thus, in addition to performing the tests as a fluorescence sensor, the Eu^{3+}@RIO-55 was used to detect ephedrine and dopamine (Fig. 1), known among doping substances, which cannot be found in excess in the body to carry out certain sports activities. This way, 10 mg of RIO-55 was added to 10 mL of $EuCl_3$ (50 ppm, Milli-Q water) and the mixture remained for 24h in a shaker (2400 rpm). As previously done, the suspension was filtered using filters attached to syringes, and the liquid was analyzed by ICP. The resulting wet solid (Eu^{3+}@RIO-55) was filtered by vacuum. Then, 4 mg of RIO-55 was added to 4 mL of an ephedrine solution (100 ppm, ethanol) and 4 mL of a dopamine solution (100 ppm, ethanol), separately. The same procedure was executed for Eu^{3+}@RIO-55 to observe the difference in the absorption values.

5. Results and discussion

RIO-55 was obtained as previously reported and all the physical-chemical characterizations are present in the ESI. In summary, N_2
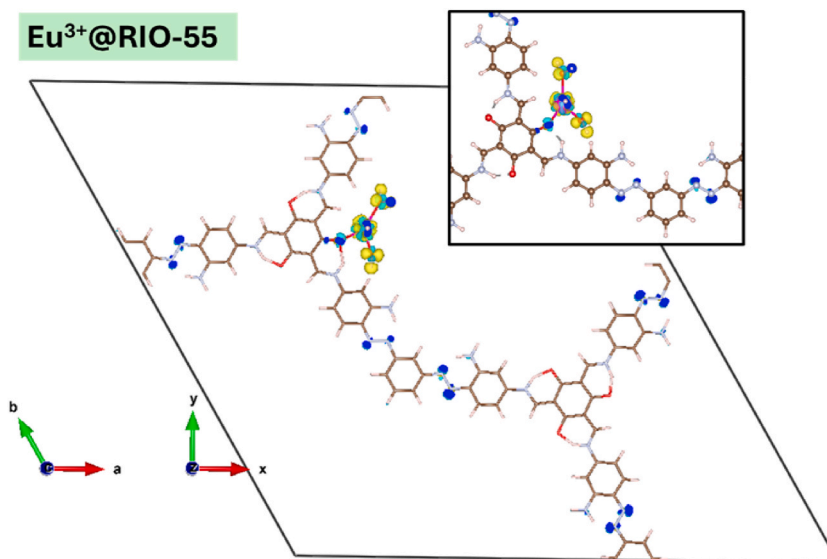
Fig. 3. DFT calculation for the impregnated Eu^{3+}@RIO-55. The high density of interaction shows the preference for oxygen atoms, even from the water molecules. Besides, there is a growing increase in density near the diazo groups.

adsorption/desorption for RIO-55 showed a type IV isotherm, indicating the presence of mesopores (~35 Å). The surface area (S_{BET}) was calculated as 420 m^2/g, which is high if compared to other ionic mesoporous materials. The pattern PXRD indicated that RIO-55 presents a low crystallinity profile, which can be explained by the charge repulsion (Cl-ions), favoring a turbostratic disorder, as found in previous works [22,32]. The peak at 28° is suggestive of a lamellar structure typical of bidimensional materials (see ESI).

Adsorption curves were obtained for each one of the lanthanides captured by RIO-55. All the isotherms were calculated following Langmuir parameters, being classified as of the favorable type (Fig. 2). RIO-55 captured a greater amount of Eu^{3+} (Q_{max} = 370 mg/g) than the other lanthanides, presenting a better affinity to the adsorbent (K_L = 0.005), besides the lanthanide contraction. This can be explained by the intraparticle diffusion (transfer of solute in the solution to the adsorbent) or by the negative steric effect on coordination. It is possible to identify this behavior from the isotherms in the initial points, showing the capture by larger pores, i.e., a faster diffusion step [33]. For a better understanding of the great amount of Eu adsorbed, it was calculated the weight of Eu per mol of pore of RIO-55, resulting in 115g of Eu/mol of pore (see ESI). Besides, RIO-55 adsorbed a good amount of Gd^{3+} (285 mg/g), Tb^{3+} (160 mg/g), and Dy^{3+} (200 mg/g). All the Langmuir fittings (non-linearized forms) are present in the ESI. Due to its large pore size (35 Å), this nanoporous material can capture a greater number of fluids, such as biomolecules, ions, metals, and metalloids. In addition, the structure of RIO-55 is composed of many N and O atoms, which increases the selectivity for these rare earth metals. These compounds can strongly attach via these sites which affect the complex stability. As observed, there is not a linear trend when comparing the ion size with the affinity in the adsorption or the amount captured. This non-linear trend obtained for lanthanides is due to other forces besides the ionic radii, as well as geometry, and steric effects of all the systems, for example.

To better understand this discussion, DFT calculations were conducted to provide a comprehensive comparison and perspective on the results. Europium is the most reactive metal among the lanthanides, seeking to interact quickly with available oxygen atoms [34–36]. According to the theoretical calculations carried out, europium has a great preference for the oxygen atoms of the keto-enamine groups and water (Fig. 3). The other lanthanides studied here also form strong interactions with other elements present in the structure of RIO-55, but less intensely than europium. However, a higher density of interaction is observed between the europium ion and water, suggesting a chemisorption that can be reversed, as observed experimentally during the reuse process. The methodology for the DFT calculation is presented in ESI.

Similar results were found for other lanthanides, such as La (III) e Sm (III), adsorbed by hydroxyapatite with Qmax = 200–400 mg/g[37]. On the other hand, Nitrolite captured only 5 mg/g of La (III); the doped silica sol-gel with a bifunctionalized ionic liquid adsorbed ~9 mg/g of Eu(III). A carbonaceous material (C-IOP) obtained a Q_{max} = 14,5 mg/g for Eu(III) [37–40]. However, there are few cases of capture of lanthanides from water. Making discussion in a comparative way with other adsorbents, RIO-55 is more suitable due to its stability and robustness (covalent bonds), besides its highly porous matrix, being an ionic framework. This materials class has been used in the capture of metals, ions, and organic compounds, among others, whose results are promising.

The effect of the pH of the medium on the adsorption was carried out using $EuCl_3$ as adsorbate. The results show that the best performance is obtained in a neutral or slightly acidic medium, i.e., as carried out in the first tests (Fig. S05). This behavior occurs at higher pH values, where Eu^{3+} ions can compete with hydrogen ions. On the other hand, the solution with lower pH values implies an effect of hydroxyl groups, decreasing the interaction by the adsorbent. The same occurred with the functionalized resin poly (amidoxime-hydroxamic) acid, an N-, O-rich structure, where the higher amount was adsorbed at pH = 7 for different lanthanides [41].

From the selectivity tests, it was noticed that the absorbed amount of each lanthanide decreased concerning the tests made

Table 1

Selectivity of the lanthanides in the competitive environment.

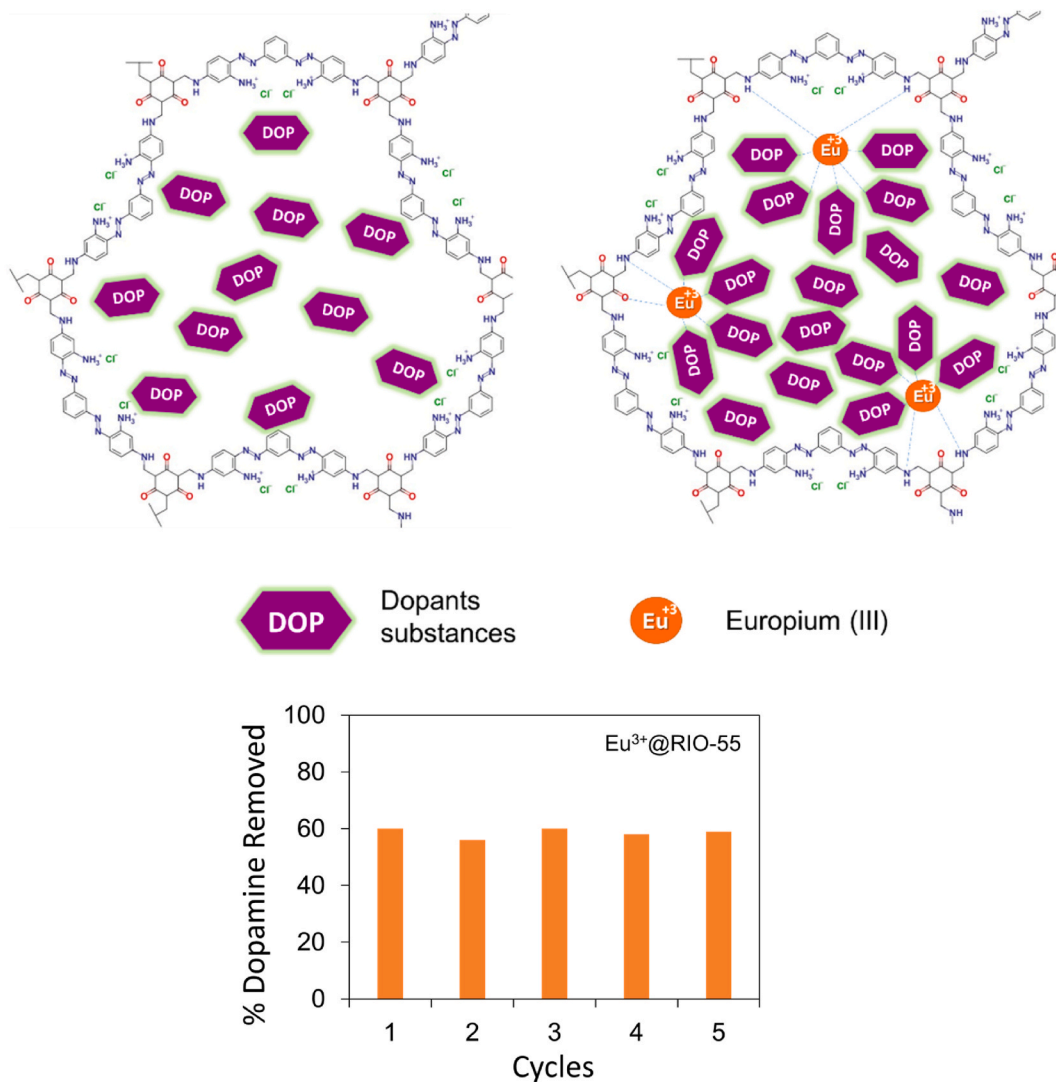|	Absorbed amount (ppm)	
Lanthanides	Non-competitive environment (100 ppm)	Competitive environment (100 ppm)
Eu	62.6	22.2
Dy	30.6	19.7
Gd	21	19.8
Tb	20.8	18

Fig. 4. Adsorption of the dopant molecules by RIO-55 (left) and by RIO-55@Eu^{3+} (right), being represented by dopamine. In the bottom, the dopamine amount was removed for 5 cycles.

separately (described above). However, the percentage of Gd^{3+} and Tb^{3+} in an environment with and without competition was similar, as shown in the table below. This can be interpreted by the fact that these ions are bigger than Eu and Dy. Then, more interactions occur with the smaller ions, and more interactions occur with the smaller ions faster more interactions occur with the smaller ions in a faster way (Table 1).

From these data, Eu^{3+}@RIO-55 was selected for some initial tests as a proof of concept to understand its fluorescence characteristics after the impregnation. These properties can open new strategies of applications, such as fluorescence sensors. The emission curves show that RIO-55 emits lower fluorescence, which increases with the presence of Eu(III) in the lattice (Fig. S04). These tests were performed with the same powdered masses for both samples (4 mg). It is observed that the bands at 420 and 440 nm are higher for

the Eu^{3+}@RIO-55. These bands can occur due to the reticulated extended structure forming a large π-conjugated system, which results in electro-relocation, besides transitions of π*→π type [22].

Eu^{3+}@RIO-55 was used as a detector for determining doping substances (ephedrine and dopamine). Tests were performed using RIO-55 and Eu^{3+}@RIO-55 to compare the adsorption efficiency with and without lanthanide. The solutions were analyzed by UV–vis and it was possible to obtain the final concentration values from the absorption bands. RIO-55 trapped 47 mg/g of ephedrine (or 47 %), while Eu^{3+}@RIO-55 adsorbed 72 mg/g (or 72 %). This shows that Eu^{3+}@RIO-55 obtained the best performance, e.g., the presence of Eu(III) impregnated in the network increased the amount absorbed (Fig. 4). The same occurred for dopamine, where RIO-55 captured 60 mg/g (or 60 %) and Eu^{3+}@RIO-55 adsorbed 82 mg/g (or 82 %). The greater adsorption of dopamine may be due to its chemical structure, having more hydrogenated groups. On the other hand, ephedrine has methyl groups, with fewer possible interactions. Eu(III) prefers to interconnect with –OH and –NH_2 functional groups, which are more available in dopamine molecules. It is interesting to notice that the europium coupled to the organic network provides even higher adsorption values than the porous structure itself. However, europium salt ($EuCl_3$) alone does not have the same result. Instead, the adsorption data are almost zero (see ESI). This chemical determination can be used as a promising technique to detect doping substances and other organic compounds.

Aiming to know the stability of the Eu^{3+}@RIO-55 as an adsorbent of dopamine, tests of reuse were performed. Fig. 4 shows good behavior, even after 5 cycles. The percentage of removal remains similar during the assays. From 100 ppm, the absorbed amount of dopamine was 60 % in 15min, presenting good stability and a considerable performance in the adsorption (Fig. 4).

6. Conclusions

In this work, RIO-55 (previously synthesized and characterized) was used as an efficient adsorbent to capture lanthanides from water, obtained great values of Q_{max} (Eu^{3+} = 370 mg/g, Gd^{3+} = 286 mg/g, Tb^{3+} = 160 mg/g and Dy^{3+} = 200 mg/g). Its large pores and chemical structure are crucial to improve the affinity with the adsorvate. From these results, some tests for fluorescence sensing were developed using RIO-55 and Eu^{3+}@RIO-55 as sensors in the solid state. The lanthanide-impregnated material showed the best performance, emitting higher fluorescence than the standard RIO-55. Moreover, Eu^{3+}@RIO-55 was also used to capture some dopant substances (ephedrine and dopamine), working as a chemical sensor. The assays were realized using the standard RIO-55 to compare the results. The affinity between Eu^{3+}@RIO-55 and the biomolecules was higher than RIO-55, due to the presence of Eu^{3+}, which can generate more interactions with the network and the dopant substances, mainly due to its structure charged by N and O atoms. Then, the impregnation of lanthanides in the lattice of porous organic materials increases the efficiency of organic substance adsorption. It was noticed that the good performance of the adsorbent after some cycles of reuse makes it a promising one. The larger pores of RIO-55 and its chemical groups in the lattice are crucial for attaching these lanthanides selectively.

Data availability

The data of this study has not been deposited into a public repository. All the information is included in the article and the supplementary material.

CRediT authorship contribution statement

André Carvalho: Formal analysis, Data curation. **Luis C. Branco:** Writing – review & editing, Validation, Methodology, Funding acquisition, Conceptualization. **Leticia R.C. Corrêa:** Theoretical calculations, data curation, writing. **Ana B. Paninho:** Writing – review & editing, Methodology. **Pierre M. Esteves:** Writing – review & editing, Funding acquisition, Data curation. **Hugo Cruz:** Supervision. **Sunny K.S. Freitas:** Writing – original draft, Validation, Supervision, Methodology, Investigation, Formal analysis, Data curation, Conceptualization.

Declaration of competing interest

The authors declare the following financial interests/personal relationships which may be considered as potential competing interests:Luis C. Branco reports financial support was provided by NOVA University Lisbon NOVA School of Science and Technology.

Acknowledgments

Appendix A. Supplementary data

Supplementary data to this article can be found online at https://doi.org/10.1016/j.heliyon.2024.e36181.

References

[1] R.D. Teo, J. Termini, H. B. Lanthanides Gray, Applications in cancer diagnosis and therapy, J. Med. Chem. 59 (13) (2016) 6012–6024, https://doi.org/10.1021/acs.jmedchem.5b01975.

[2] S. Aime, S.G. Crich, E. Gianolio, G.B. Giovenzana, L. Tei, E. Terreno, High sensitivity lanthanide(III) based probes for MR-medical imaging, Coord. Chem. Rev. (June 2006) 1562–1579, https://doi.org/10.1016/j.ccr.2006.03.015.

[3] Y. Zhang, W. Wei, G.K. Das, T.T. Yang Tan, Engineering lanthanide-based materials for nanomedicine, J. Photochem. Photobiol. C Photochem. Rev. (2014) 71–96, https://doi.org/10.1016/j.jphotochemrev.2014.06.001. Elsevier.

[4] K. Binnemans, Lanthanide-based luminescent hybrid materials, Chem Rev 109 (9) (2009) 4283–4374, https://doi.org/10.1021/cr8003983.

[5] D. Kim, K.T. Lee, Effect of lanthanide (Ln=La, Nd, and Pr) doping on electrochemical performance of Ln2NiO4+δ−YSZ composite cathodes for solid oxide fuel cells, Ceram. Int. 47 (2) (2021) 2493–2498, https://doi.org/10.1016/j.ceramint.2020.09.092.

[6] M. Jia, Z. Sun, M. Zhang, H. Xu, Z. Fu, What determines the performance of lanthanide-based ratiometric nanothermometers? Nanoscale 12 (40) (2020) 20776–20785, https://doi.org/10.1039/D0NR05035K.

[7] K. Binnemans, C. Görller-Walrand, Lanthanide-containing liquid crystals and surfactants, Chem Rev 102 (6) (2002) 2303–2346, https://doi.org/10.1021/cr010287y.

[8] X. Gao, G. Sun, F. Ge, H. Zheng, Three anionic indium–organic frameworks for highly efficient and selective dye adsorption, lanthanide adsorption, and luminescence regulation, Inorg. Chem. 58 (13) (2019) 8396–8407, https://doi.org/10.1021/acs.inorgchem.9b00499.

[9] E.L. Afonso, L. Carvalho, S. Fateixa, C.O. Amorim, V.S. Amaral, C. Vale, E. Pereira, C.M. Silva, T. Trindade, C.B. Lopes, Can contaminated waters or wastewater Be alternative sources for technology-critical elements? The case of removal and recovery of lanthanides, J. Hazard Mater. 380 (2019), https://doi.org/10.1016/j.jhazmat.2019.120845.

[10] R. Li, B. Wang, A. Niu, N. Cheng, M. Chen, X. Zhang, Z. Yu, S. Wang, Application of biochar immobilized microorganisms for pollutants removal from wastewater: a review, Sci. Total Environ. (2022), https://doi.org/10.1016/j.scitotenv.2022.155563. Elsevier B.V. September 1.

[11] M.T. Amin, A.A. Alazba, U. Manzoor, A review of removal of pollutants from water/wastewater using different types of nanomaterials. Advances in Materials Science and Engineering, Hindawi Publishing Corporation, 2014, https://doi.org/10.1155/2014/825910.

[12] Q. Ren, P. Yang, J. Liu, Y. Chen, S. Ouyang, Y. Zeng, P. Zhao, J. Tao, An imine-linked covalent organic framework for renewable and sensitive determination of antibiotic, Anal. Chim. Acta 1188 (2021), https://doi.org/10.1016/j.aca.2021.339191.

[13] M. Safdar, A. Ghazy, M. Lastusaari, M. Karppinen, Lanthanide-based inorganic–organic hybrid materials for photon-upconversion, J Mater Chem C Mater 8 (21) (2020) 6946–6965, https://doi.org/10.1039/D0TC01216E.

[14] M. Sun, G. Chen, S. Ouyang, C. Chen, Z. Zheng, P. Lin, X. Song, H. Chen, Y. Chen, Y. You, J. Tao, B. Lin, P. Zhao, Magnetic resonance diagnosis of early triple-negative breast cancer based on the ionic covalent organic framework with high relaxivity and long retention time, Anal. Chem. 95 (21) (2023) 8267–8276, https://doi.org/10.1021/acs.analchem.3c00307.

[15] A.P. Cote, Porous, crystalline, covalent organic frameworks, Science 310 (5751) (2005) 1166–1170, https://doi.org/10.1126/science.1120411, 1979.

[16] P.J. Waller, F. Gándara, O.M. Yaghi, Chemistry of covalent organic frameworks, Acc. Chem. Res. (2015), https://doi.org/10.1021/acs.accounts.5b00369 acs.accounts.5b00369.

[17] Z. Xia, Y. Zhao, S.B. Darling, Covalent organic frameworks for water treatment, Adv Mater Interfaces 8 (1) (2021) 1–17, https://doi.org/10.1002/admi.202001507.

[18] Y. Zeng, R. Zou, Y. Zhao, Covalent organic frameworks for CO2 capture, Adv. Mater. 28 (2016) 2855–2873, https://doi.org/10.1002/adma.201505004.

[19] H. Hu, Q. Yan, R. Ge, Y. Gao, Covalent organic frameworks as heterogeneous catalysts, Chin. J. Catal. 39 (7) (2018) 1167–1179, https://doi.org/10.1016/S1872-2067(18)63057-8.

[20] D.D. Medina, T. Sick, T. Bein, Photoactive and conducting covalent organic frameworks, Adv. Energy Mater. 7 (16) (2017) 1–8, https://doi.org/10.1002/aenm.201700387.

[21] J. Zou, K. Fan, W. Hu, C. Wang, Perspectives of ionic covalent frameworks for rechargeable batteries, Coord. Chem. Rev. 458 (2022) 214431.

[22] S.K.S. Freitas, F.L. Oliveira, C. Merlini, E.P.S. Justo, A. Gioda, P.M. Esteves, Dye-based covalent organic networks (CONs), J. Phys.: Materials 3 (2020) 025011, https://doi.org/10.1088/2515-7639/ab854b.

[23] Y. Peng, Y. Huang, Y. Zhu, B. Chen, L. Wang, Z. Lai, Z. Zhang, M. Zhao, C. Tan, N. Yang, F. Shao, Y. Han, H. Zhang, Ultrathin two-dimensional covalent organic framework nanosheets: preparation and application in highly sensitive and selective DNA detection, J. Am. Chem. Soc. 139 (25) (2017) 8698–8704, https://doi.org/10.1021/jacs.7b04096.

[24] G. Das, B.P. Biswal, S. Kandambeth, V. Venkatesh, G. Kaur, M. Addicoat, T. Heine, S. Verma, R. Banerjee, Chemical sensing in two dimensional porous covalent organic nanosheets, Chem. Sci. 6 (7) (2015) 3931–3939, https://doi.org/10.1039/c5sc00512d.

[25] R.A. Maia, F.L. Oliveira, M. Nazarkovsky, P.M. Esteves, Crystal engineering of covalent organic frameworks based on hydrazine and hydroxy-1,3,5-triformylbenzenes, Cryst. Growth Des. 18 (2018) 5682–5689.

[26] C.J.F. Oliveira, S.K.S. Freitas, I.G.P.P. de Sousa, P.M. Esteves, R.A. Simao, Solvent role on covalent organic framework thin film formation by ultrasound, Colloids Surf. A Physicochem. Eng. Asp. 585 (JANUARY 2) (2019) 124086, https://doi.org/10.1016/j.colsurfa.2019.124086.

[27] G.W. Kajjumba, E.J. Marti, A review of the application of cerium and lanthanum in phosphorus removal during wastewater treatment: characteristics, mechanism, and recovery, Chemosphere 1 (2022), https://doi.org/10.1016/j.chemosphere.2022.136462. Elsevier Ltd December.

[28] N. Kasera, P. Kolar, S.G. Hall, Nitrogen-doped biochars as adsorbents for mitigation of heavy metals and organics from water: a review, Biochar (2022), https://doi.org/10.1007/s42773-022-00145-2. Springer December 1.

[29] S. Armaković, S.J. Armaković, B.T. Tomić, R.R. Pillai, C.Y. Panicker, Adsorption properties of graphene towards the ephedrine – a frequently used molecule in sport, Comput Theor Chem 1124 (2018) 39–50, https://doi.org/10.1016/j.comptc.2017.12.009.

[30] I. Urdaneta, A. Keller, O. Atabek, J.L. Palma, D. Finkelstein-Shapiro, P. Tarakeshwar, V. Mujica, M. Calatayud, Dopamine adsorption on TiO_2 anatase surfaces, J. Phys. Chem. C 118 (35) (2014) 20688–20693, https://doi.org/10.1021/jp506156e.

[31] Q. Ren, H. Chen, Y. Chen, Z. Song, S. Ouyang, S. Lian, J. Tao, Y. Song, P. Zhao, Imine-linked covalent organic framework modulates oxidative stress in alzheimer's disease, ACS Appl. Mater. Interfaces 15 (4) (2023) 4947–4958, https://doi.org/10.1021/acsami.2c19839.

[32] S.K.S. Freitas, F.L. Oliveira, T.C. Dos Santos, D. Hisse, C. Merlini, C. Machado, P.M. Esteves, A carbocationic triarylmethane-based porous covalent organic network, Chem. Eur J. 27 (2020) 2342, https://doi.org/10.1002/chem.202003554.

[33] C. Noureddine, A. Lekhmici, M.S. Mubarak, Sorption properties of the iminodiacetate ion exchange resin, amberlite IRC-718, toward divalent metal ions, J. Appl. Polym. Sci. 107 (2) (2008) 1316–1319, https://doi.org/10.1002/app.26627.

[34] S.M. Borisov, R. Fischer, R. Saf, I. Klimant, Exceptional oxygen sensing properties of new blue light-excitable highly luminescent europium(III) and gadolinium (III) complexes, Adv. Funct. Mater. 24 (41) (2014) 6548–6560, https://doi.org/10.1002/adfm.201401754.

[35] E. Heyduk, T. Heyduk, E.A. Doisy, Thiol-Reactive, Luminescent Europium Chelates: Luminescence Probes for Resonance Energy Transfer Distance Measurements in Biomolecules 248 (1997), https://doi.org/10.1006/abio.1997.2148.

[36] D. Wang, Z. Luo, Z. Liu, D. Wang, L. Fan, G. Yin, Synthesis and photoluminescent properties of Eu (III) complexes with fluorinated β-diketone and nitrogen heterocyclic ligands, Dyes Pigments 132 (2016) 398–404, https://doi.org/10.1016/j.dyepig.2016.05.026.

[37] I.M. Ali, M. Khalil, H.A. Madbouly, A.M. Soliman, Efficient lanthanides adsorption using magnetic hydroxyapatite incorporated cobalt, Int. J. Environ. Anal. Chem. 1–20 (2021), https://doi.org/10.1080/03067319.2021.1912332.

[38] A.N. Turanov, V.K. Karandashev, N.S. Sukhinina, V.M. Masalov, A.A. Zhokhov, G.A. Emelchenko, A novel sorbent for lanthanide adsorption based on tetraoctyldiglycolamide, modified carbon inverse opals, RSC Adv. 5 (1) (2015) 529–535, https://doi.org/10.1039/c4ra11999a.

[39] A.N. Turanov, V.K. Karandashev, N.S. Sukhinina, V.M. Masalov, G.A. Emelchenko, Adsorption of lanthanides and scandium ions by silica sol-gel material doped with novel bifunctional ionic liquid, trioctylmethylammonium 1-phenyl-3-methyl-4-benzoyl-5-onate, J. Environ. Chem. Eng. 4 (4) (2016) 3788–3796, https://doi.org/10.1016/j.jece.2016.08.024.

[40] G. Wójcik, Sorption behaviors of light lanthanides(III) (La(III), Ce(III), Pr(III), Nd(III)) and Cr(III) using nitrolite, Materials 13 (10) (2020) 2256, https://doi.org/10.3390/ma13102256.

[41] F. Alakhras, Kinetic studies on the removal of some lanthanide ions from aqueous solutions using amidoxime-hydroxamic acid polymer, J Anal Methods Chem 2018 (2018), https://doi.org/10.1155/2018/4058503.